($H_2OFeCl_2^+$) and 179, 181, 183 ($H_2OFeCl_3^+$), along with ions expected from $FeCl_3$ and Fe_2Cl_6, were observed. At about 1 min mass peak 91 ($FeCl^+$) had the maximum intensity and the 109 peak a relative intensity of 19%. Around 2 min the 254 peak ($Fe_2Cl_4^+$) had maximum intensity, with 109 at 40%. After about 3 min the hydrate peaks had essentially merged into the background, to be expected after water vapor and hydrogen chloride have been removed by the vacuum system. Ions from the iron(III) chloride molecules persisted somewhat longer. The second sample duplicated the behavior observed with the first. Ions that could be identified exclusively as formed by parent molecules, such as $Fe_2(OH)_2Cl_4$ or related hydroxy halide dimers, were not above background level. While such molecules might, nevertheless, be important in the equilibrium systems, their presence does not seem to be required to explain the absorbance and mass spectrometric behavior observed in the present study. Mass spectrometric evidence for the presence of traces of oxy and hydroxy chlorides of aluminum in aluminum chloride vapor in contact with quartz or glass[8] and traces of hydroxy chlorides of iron in iron(III) chloride vapor containing small amounts of water as an impurity[9] has recently been reported.

A_x Absorption Spectrum in the Range 250–600 nm. The absence of appreciable photolytic effects and the position of the absorption peak maximum around 340 nm for vapors of samples 5–7 indicate that Fe_2Cl_6 and $FeCl_3$ contribute to the total absorbance in only a minor way. A_x values at various wavelengths from data from sample 7 at 280 °C were converted to estimated molar absorptivities by using a concentration based on the estimated value $E_x = 5000$ M^{-1} cm^{-1} at 360 nm, comparable to values for $FeCl_3$[10] and NH_3FeCl_3.[11] The resulting spectrum is shown in Figure 3 in comparison with spectra of other iron(III) chloride vapor molecules. The A_x spectrum is very similar to that reported for NH_3FeCl_3[11] and is believed to be associated with charge-transfer transitions. The bonding and structure of H_2OFeCl_3 and H_3NFeCl_3 would be expected to be similar, with the iron atom bonded to three chlorine atoms and an oxygen (or nitrogen) atom in an approximately tetrahedral configuration. The concentration estimated indicates that the iron in the vapor of this sample is largely in the form of the hydrate molecule; the derived ratio $P_x/(P_x + P_D + P_M)$, where P_x is the partial pressure of H_2O-$FeCl_3$, is 0.9. For the mixtures included in Figure 1a this ratio varies from 0.4 to nearly unity and shows a general correlation with the shift in the wavelength of the absorption peak maximum. Ratios will be smaller if E_x is actually larger than the assumed value.

Estimated Thermodynamic Properties. The estimated molar absorptivity, temperature dependence neglected, together with the equilibrium constant expressions derived above give, for reaction 4, $\Delta G_4° = 37 + 13.44T$ cal mol^{-1} and, for reaction 6, $\Delta G_6° = -10244 + 51.02T$ cal mol^{-1}. Together with thermodynamic constants for the other substances in reactions 4 and 6 taken from references cited above, the constants in these free energy equations give −141 kcal mol^{-1} for the standard enthalpy of formation and 113 cal mol^{-1} deg^{-1} for the standard entropy of $H_2OFeCl_3(g)$ at 500 K. These values seem reasonable although data for similar hydrate vapor molecules have not been found for comparison. The derived entropy is, of course, sensitive to the uncertainty of the value estimated for E_x. The result projects, for example, for the dissociation reaction $H_2OFeCl_3(g) = FeCl_3(g) + H_2O(g)$, $\Delta G° = 22000 - 29.0T$ cal mol^{-1}, which may be compared with $\Delta G° = 34550 - 34.0T$ cal mol^{-1} for $Fe_2Cl_6(g) = 2FeCl_3(g)$. In the latter case dissociation requires the rupture of two Fe–Cl bridge bonds as compared with a single Fe–O bond in the former, assuming the proposed structure.

Registry No. Fe_2O_3, 1309-37-1; $FeCl_3$, 7705-08-0; H_2OFeCl_3, 60684-13-1; HCl, 7647-01-0.

(9) Naumova, T. N.; Zhevnina, L. S.; Poponova, R. V.; Chupakhjin, M. S.; Stepin, B. D. *Russ. J. Inorg. Chem.* (*Engl. Transl.*) **1979**, *24*, 10.
(10) Rustad, D. S.; Gregory, N. W. *Inorg. Chem.* **1977**, *16*, 3036.
(11) Gregory, N. W. *Inorg. Chem.* **1981**, *20*, 3667.
(12) Results of a subsequent study (with D. S. Rustad) of mixtures with much lower partial pressures of water correlate better with present data when the condensed hydrate phase is assumed to be $FeCl_3(H_2O)$. This indicates tht the improved correlation noted in this paragraph, using $FeCl_3(H_2O)_{0.5}$, may not be significant relative to overall experimental error.

Contribution from the Departments of Chemistry, Wayne State University, Detroit, Michigan 48202, and Illinois Institute of Technology, Chicago, Illinois 60616

Electron-Transfer Reactivity in Some Simple Cobalt(III)–Cobalt(II) Couples. Franck–Condon vs. Electronic Contributions[1]

JOHN F. ENDICOTT,*† GEORGE R. BRUBAKER,*†‡ T. RAMASAMI,† KRISHAN KUMAR,† KADDI DWARAKANATH,† JONATHAN CASSEL,† and DAVID JOHNSON‡

Received August 9, 1982

Electron-transfer rates involving the $Co(sep)^{3+,2+}$ (sep = 1,3,6,8,10,13,16,19-octaazabicyclo[6.6.6]eicosane) and $Co(en)_3^{3+,2+}$ couples have been examined for any differences in contributions of Franck–Condon and electronic terms to the rate constants. Rate constants for cross-reaction oxidations of $Co(sep)^{2+}$ follow the classically predicted dependence of the Franck–Condon factor on $\Delta G_{ab}°$. Far-infrared and Raman vibrational spectra of $M(sep)^{3+}/M(en)_3^{3+}$ (M = Co, Rh) are in very close correspondence. As a consequence, the force constants of the M–N stretching modes must also be comparable (differing by less than 10%) in the $Co(sep)^{3+}$ and $Co(en)_3^{3+}$ complexes. Strain energy calculations based on these and other published force constants are consistent with the differences in self-exchange rates and indicate upper limits on the Franck–Condon term in the rate constants consistent with significant contributions from electronic factors in both exchange reactions.

Introduction

A current concern in the study of electron-transfer reactivity relates to the significance of donor–acceptor electronic interactions in determining reactivity.[2-17] Thus, the bimolecular rate constant may be formulated[2-6,8]

$$k = K_o\nu^2[G(FC)]$$

† Wayne State University.
‡ Illinois Institute of Technology.

(1) Partial support of this research by the National Institutes of Health (Grant No. AM 14341) and by the Department of Energy (Grant No. ER-78-S-02-4685) is gratefully acknowledged.

0020-1669/83/1322-3754$01.50/0

where, in nonadiabatic processes, the electronic component is given by[2-6]

$$\nu \simeq \nu^0 \exp(-\alpha r_{DA}) \quad (1)$$

In most electron-transfer reactions the Franck–Condon factor, G(FC), governs the major features of reactivity patterns and the contributions of purely electronic terms are very difficult to establish.[2,4,5-7,9-12] We have been examining reactivity patterns of Co(III)–Co(II) couples in an attempt to document the Franck–Condon factors.[10-12] One might hope that a quantitative comparison of these factors to the observed rates could be used to establish the significance of electronic contributions to reactivity. Owing to changes in spin multiplicity, possibly poor σ^*–σ^* donor–acceptor overlap, and the large bond length changes accompanying electron transfer in Co(III)–Co(II) couples,[12,13] one might expect that electron-transfer reactions of cobalt systems will be among the most nonadiabatic.[4d,12,13] It has, therefore, been of particular interest that Co(III)–Co(II) couples have often been (1) found to exhibit vastly different self-exchange rates for very similar complexes (e.g., $Co(NH_3)_6^{3+,2}$[14] compared to $Co(OH_2)_6^{3+,2+}$,[15] $Co(en)_3^{3+,2+}$[16,17] compared to $Co(sep)^{3+,2+}$[18]), (2) alleged[19-22] to exhibit free energy dependencies other than predicted,[23] and (3) frequently found to be "nonadiabatic".[4d,7-12] Many of the most dramatic peculiarities of these systems have vanished upon acquisition of crucial structural, vibrational, or thermochemical data and upon closer examination of kinetic data.[12,23] Thus, deviations from the classically predicted dependence on $\Delta G_{ab}°$[24]

$$\Delta G_{ab}^{\ddagger} = w_{ab} + \frac{1}{2}\Delta G_{ab}° + \frac{(\Delta G_{ab}°)^2}{4\lambda_{ab}} + \frac{\lambda_{ab}}{4} \quad (2)$$

have often been found to be a consequence of errors in self-exchange or free energy parameters used or a consequence of failure to take proper account of the variation in reorganizational parameters (λ_{ab}). Furthermore, evidence has recently been found[11] that the outer-sphere self-exchange parameters are similar and very small for $Co(NH_3)_6^{3+,2+}$ and $Co(OH_2)_6^{3+,2+}$, with the "experimentally determined" value for the $Co(OH_2)_6^{3+,2+}$ exchange probably corresponding to a water-bridged, inner-sphere reaction. Although the 5 orders of magnitude difference in the $Co(en)_3^{3+,2+}$ and $Co(sep)^{3+,2+}$ self-exchange rates at one time led to speculation about the inadequacy of Franck–Condon models,[18b] more recently this contrast in the intrinsic reactivity of two very similar couples has been variously ascribed to a large difference in the critical vibrational frequencies[10,25] or to a relief of ground-state strain energy in the $Co(sep)^{3+,2+}$ electron-transfer transition state.[26] Our study has had two goals. One was to make a more critical examination of the Franck–Condon contributions to the $Co(en)_3^{3+,2+}$ and $Co(sep)^{3+,2+}$ self-exchange reactions, and the second was to examine reactions of these complexes for contributions of electronic factors.

Experimental Section

Chemicals and Reagents. Literature methods were used for the synthesis of $Co(NH_3)_6Cl_3$,[27] $Co(en)_3Cl_3$,[28] and $Co(bpy)_3Cl_3$.[29] $Co(sep)Cl_3$ was prepared by a variation on methods described earlier:[18,30] A solution containing 5 g of $Co(en)_3Cl_3$ in 60 mL of water was combined with 30 mL of formalin, and the mixture was cooled in an ice bath to ~5 °C. Ammonia gas was passed through the cooled solution sufficiently slowly that the temperature remained below 15 °C. After ~90 min the ammonia was stopped, and concentrated HCl was added dropwise until pH ~5. The resulting mixture was warmed to room temperature and then concentrated to ~50 mL on a steam bath. Ethanol, 100–200 mL, was added to the cooled solution until turbidity began to develop. The mixture was filtered, and the filtrate was warmed to 50 °C and then cooled slowly. After it was cooled to room temperature, the mixture was refrigerated for 1–2 days. The solid product was collected by filtration and washed with ice-cold water, ethanol, and ether. The product was recrystallized by dissolving the solid in a minimum volume of 0.5 M HCl and then adding 3 volumes of ethanol to the solution and cooling. The sample of $Rh(sep)Cl_3$ was kindly prepared for us by Dr. D. C. Gaswick using a variation of this procedure.

(2) Brunschwig, B. S.; Logan, J.; Newton, M. D.; Sutin, N. *J. Am. Chem. Soc.* **1980**, *102*, 5798.
(3) (a) Newton, M. D. *Int. J. Quantum Chem., Quantum Chem. Symp.* **1980**, *No. 14*, 363. (b) Newton, M. D. *ACS Symp. Ser.* **1982**, *No. 198*, 255.
(4) (a) Ulstrup, J.; Jortner, J. *J. Chem. Phys.* **1975**, *63*, 4358. (b) Kestner, N. R.; Logan, J.; Jortner, J. *J. Phys. Chem.* **1974**, *78*, 2148. (c) Jortner, J.; Ulstrup, J. *J. Am. Chem. Soc.* **1979**, *101*, 3744. (d) Buhks, E.; Bixon, M.; Jortner, J.; Navon, G. *Inorg. Chem.* **1979**, *18*, 2014. (e) Buhks, E.; Bixon, M.; Jortner, J.; Navon, G. *J. Phys. Chem.* **1981**, *85*, 3759.
(5) Buhks, E.; Wilkins, R. G.; Isied, S. S.; Endicott, J. F. *ACS Symp. Ser.* **1982**, *No. 198*, 213.
(6) (a) Sutin, N.; Brunschwig, B. S. *ACS Symp. Ser.* **1982**, *No. 198*, 105. (b) Sutin, N. *Acc. Chem. Res.* **1982**, *15*, 275.
(7) (a) Endicott, J. F.; Heeg, M. J.; Gaswick, D. C.; Pyke, S. C. *J. Phys. Chem.* **1981**, *85*, 1777. (b) Endicott, J. F.; Ramasami, T. *J. Am. Chem. Soc.* **1982**, *104*, 5252.
(8) Implicit in k is a summation over all nuclear configurations and electronic states. G(FC) is the Franck–Condon factor, K_0 is an outer-sphere association constant, ν^2 is an effective frequency term based on the vibronic matrix element, α can be most simply interpreted as an inverse mean orbital radius, and r_{DA} is the mean distance of closest approach of the donor and acceptor.
(9) (a) Chou, M.; Creutz, C.; Sutin, N. *J. Am. Chem. Soc.* **1977**, *99*, 5615. (b) Brown, G.; Sutin, N. *Ibid.* **1979**, *101*, 883.
(10) Endicott, J. F.; Durham, B.; Glick, M. D.; Anderson, T. J.; Kuszaj, J. M.; Schmonsees, W. G.; Balakrishnan, K. P. *J. Am. Chem. Soc.* **1981**, *103*, 1431.
(11) Endicott, J. F.; Durham, B.; Kumar, K. *Inorg. Chem.* **1982**, *21*, 2437.
(12) Endicott, J. F.; Kumar, K.; Ramasami, T.; Rotzinger, F. P. *Prog. Inorg. Chem.* **1983**, *30*, 142.
(13) In general one expects the reactions that are accompanied by large bond length changes to be the reactions most sensitive to electronic factors owing to the relatively higher frequencies of metal–ligand ($\sim 10^{-13}$ s^{-1}) than of solvent vibrations. Thus, for the effectiveness of reactant–product coupling at the Franck–Condon crossing point described semiclassically by the Landau–Zener model for surface crossing, the transmission coefficient is given by[2,3,6]

$$\kappa = 2(1 - \exp(-\nu_{el}/2\nu_n))/(2 - \exp(-\nu_{el}/2\nu_n))$$

where ν_{el} and ν_n are the effective frequencies of electronic and nuclear motion, respectively.
(14) (a) Stranks, D. R. *Discuss. Faraday Soc.* **1960**, *29*, 73. (b) Birader, N. S.; Stranks, D. R.; Vaidya, M. S. *Trans. Faraday Soc.* **1962**, *58*, 2421.
(15) Habib, H. S.; Hunt, J. P. *J. Am. Chem. Soc.* **1966**, *88*, 1668.
(16) Lewis, N. B.; Coryell, C. D.; Irvine, J. W. *J. Chem. Soc.* **1949**, 5386.
(17) Dwyer, F. P.; Sargeson, A. M. *J. Phys. Chem.* **1961**, *65*, 1892.
(18) (a) Creaser, I. I.; Harrowfield, J. M.; Herit, A. J.; Sargeson, A. M.; Springborg, J.; Geue, R. J.; Snow, M. R. *J. Am. Chem. Soc.* **1977**, *99*, 3181. (b) Sargeson, A. M. *Chem. Br.* **1979**, *15*, 23. (c) Creaser, I. I.; Geue, R. J.; Harrowfield, J. M.; Herit, A. J.; Sargeson, A. M.; Snow, M. R.; Springborg, J. *J. Am. Chem. Soc.* **1982**, *104*, 6016.
(19) (a) Rillema, D. P.; Endicott, J. F.; Patel, R. C. *J. Am. Chem. Soc.* **1972**, *94*, 394. (b) Rillema, D. P.; Endicott, J. F. *Ibid.* **1972**, *94*, 8711. (c) Rillema, D. P.; Endicott, J. F. *Inorg. Chem.* **1972**, *11*, 2361.
(20) (a) Davies, G.; Warnquist, B. *Coord. Chem. Rev.* **1970**, *5*, 349. (b) Bodek, I.; Davies, G. *Ibid.* **1974**, *14*, 269. (c) Davies, G. *Ibid.* **1974**, *14*, 287. (d) Davies, G. *Inorg. Chem.* **1971**, *10*, 1155.
(21) Hyde, M. R.; Davies, R.; Sykes, A. G. *J. Chem. Soc., Dalton Trans.* **1972**, 1838.
(22) Ekstrom, A.; McLaren, A. B.; Smythe, L. E. *Inorg. Chem.* **1975**, *14*, 2899.
(23) (a) Taube, H. "Abstracts of Papers", 183rd National Meeting of the American Chemical Society, Las Vegas, NV, March 1982; American Chemical Society: Washington, DC, 1982; INOR 121. (b) Geselowitz, D.; Taube, H. *Adv. Inorg. Bioinorg. Mech.* **1982**, *1*, 391.
(24) (a) Marcus, R. A. *Annu. Rev. Phys. Chem.* **1964**, *15*, 155. (b) Marcus, R. A. *J. Phys. Chem.* **1963**, *67*, 853. (c) Marcus, R. A. *Discuss. Faraday Soc.* **1960**, *29*, 21.
(25) Geselowitz, D. *Inorg. Chem.* **1981**, *20*, 4457.
(26) (a) Pizer, R. *ACS Symp. Ser.* **1982**, *No. 198*, 127. (b) Geue, R.; Pizer, R.; Sargeson, A. M. "Abstracts of Papers", 183rd National Meeting of the American Chemical Society, Las Vegas, NV, March 1982; American Chemical Society: Washington, DC, 1982; INOR 62.
(27) Bjerrum, J.; McReynolds, J. P. *Inorg. Synth.* **1946**, *2*, 217.
(28) Bjerrum, J. *Inorg. Synth.* **1946**, *2*, 221.
(29) Nyholm, R. S. *J. Chem. Soc.* **1952**, 3570.
(30) Ferraudi, G. J.; Endicott, J. F. *Inorg. Chim. Acta* **1979**, *37*, 219.

The purity of the cobalt and rhodium sepulchrate complexes was established by elemental analysis and by electronic, infrared, and NMR spectral data. The ^1H and ^{13}C NMR spectra of $Co(sep)Cl_3$ agreed well with those reported previously.[18c] Differential pulse polarograms, recorded with a PAR 174A polarographic analyzer with hanging-mercury-drop or carbon-paste working electrodes, were also utilized in the characterization of samples of $Co(sep)^{3+}$ salts.

$Ru(NH_3)_6Cl_3$ was obtained from Johnson-Matthey, Ltd., and was purified by recrystallization.

Solutions of $Co(sep)^{2+}$ were prepared by the Zn-dust reduction of deaerated solutions of $Co(sep)Cl_3$ in sodium trifluoromethanesulfonate at pH 5.5–6.0. Reduction under our conditions took about 30 min and was monitored by observation of the electronic absorption spectra of reduced solutions and by the reducing titer as inferred from reduction of $Fe(phen)_3^{3+}$. Chromous solutions were prepared by Zn-amalgam reduction of $Cr(ClO_4)_3 \cdot xH_2O$. Solutions of reducing agents were deaerated by purging with a stream of Cr^{2+}-scrubbed N_2 or Ar and transferred by means of syringe techniques.

Trifluoromethanesulfonic acid (3 M) was redistilled at least twice before use. The sodium salt, NaO_3SCF_3, was prepared by reaction of HO_3SCF_3 with Na_2CO_3. Ionic strength was generally adjusted with NaO_3SCF_3. Deionized, redistilled water was used for all solutions.

Kinetic Methods. Rate measurements were performed for fast reactions with a thermostated Gibson-Durrum spectrophotometer and for slow reactions with a Gilford Model 250 spectrophotometer. The slow reactions of $Co(NH_3)_6^{3+}$ or $Co(en)_3^{3+}$ with $Co(sep)^{2+}$ were carried out with use of a large excess ($\geq$20-fold) of oxidant. These reactions were monitored at 260–275 nm, and the reaction solutions were $\sim 10^{-3}$ M in $[H^+]$ with $10[Co(sep)^{2+}] \leq [H^+]$. When precautions are taken to exclude O_2 and to avoid excessive increase in pH from the NH_3 or en ligands (released following reduction of the Co(III) complexes), pseudo-first-order plots were linear to between 3 and 5 half-lives and single-stage kinetics were observed. To ensure that acid decomposition of $Co(sep)^{2+}$ was not a complicating feature under the kinetic conditions, the behavior of $Co(sep)^{2+}$ in solutions of identical acid and ionic composition was examined, and [Co(III)] in the reactant solutions was adjusted such that the pseudo-first-order rate of the electron-transfer reaction would be at least 10 times faster than that of the acid decomposition of $Co(sep)^{2+}$.[18c]

With the $Co(bpy)_3^{3+}/Co(sep)^{2+}$ reactions, the range of useful concentrations was necessarily limited by poor solubilities and spectroscopic complications arising from the decomposition of $Co(bpy)_3^{2+}$ following electron transfer. We found that dissociation of $Co(bpy)_3^{2+}$ to occur with a rate constant of ca. 3 s^{-1} under our reaction conditions. Complications originating from this secondary reaction were minimized by monitoring the progress of the electron-transfer reaction at 318 nm; at this wavelength optical changes originating from $Co(bpy)_3^{2+}$ decomposition were negligible. Rate constants obtained by the usual pseudo-first-order or Guggenheim kinetic treatments agreed to within 10%. The second-order rate constants obtained for electron-transfer reactions with half-lives at least 5 times longer or shorter than the half-life for $Co(bpy)_3^{2+}$ decomposition agreed to within 15%.

All reactions were carried out under pseudo-first-order conditions. Second-order rate constants were obtained from the concentration dependence of pseudo-first-order rate constants.

Vibrational Spectra. Infrared spectra were determined in KBr matrices with a Perkin-Elmer Model 283 spectrometer. Low-frequency Raman spectra (100–600 cm^{-1}) were obtained with two different spectrometers and two different excitation frequencies. The Raman spectra of $Co(sep)^{3+}$ and of $Co(sep)^{2+}$ were obtained in aqueous sodium perchlorate solutions or in aqueous solutions with no added salt. In typical determinations solutions were $\sim 10^{-2}$ M in $Co(sep)^{3+}$ or saturated in $Co(sep)^{2+}$. For studies of the latter, the saturated solutions were prepared 0.01 M in $NaClO_4$, filtered, and transferred to a capillary under air-free conditions; solutions of $Co(sep)^{2+}$ in the sample capillaries were protected from air by sealing the capillaries under a N_2 atmosphere.

Studies of $Co(en)_3^{3+}$ have shown that, among the Raman-scattered lines, the intensity of the a_{1g} breathing mode decreases markedly as the excitation frequency increases into the range of the spin-allowed d–d transitions.[31] To obtain spectra in the 400–600-cm^{-1} region for $Co(sep)^{3+}$ and in the 350–600-cm^{-1} region for $Co(sep)^{2+}$, we used a commercial Spex spectrophotometer set at an excitation wavelength of 514.5 nm and 200–250-mW radiation intensity at the sample. Low-frequency vibrations of the $Co(sep)^{3+}$ complex, 100–450 cm^{-1}, were obtained with a system incorporating a Coherent Radiation krypton laser for excitation at 474.96 nm (with 90-mW radiation intensity at the sample), a computer-controlled scanning Jobin-Yvon double monochromator, and a photon-counting detector; scattered light intensities were stored, averaged, and processed by the computer for full 4-h spectral scans ($\Delta\nu$ from -100 to -1000 cm^{-1}).

Electrochemical Studies. Raman electrochemical studies of the $Co(sep)^{3+,2+}$ couple used the Princeton Applied Research Model 174A polarographic analyzer in the differential pulse polarographic mode, a hanging-mercury-drop electrode, and a scan rate of 10 mV s^{-1}.

In order to investigate the possibility that conformational equilibria in the $Co(sep)^{3+,2+}$ couple might complicate observations on the electrochemical time scale, we have employed the PAR system in a cyclic voltammetric configuration and used a Nicolet Explorer III digital oscilloscope to record the voltammograms with scan rates 50 mV s^{-1} to 100 V s^{-1}.

Proton NMR Spectra. Investigations employed a Nicolet 300-MHz instrument, D_2O solvent, and $[Co(III)] \approx 10^{-2}$ M.

Molecular Mechanics. The strategy described by Boyd[32] was employed in a local adaptation[33] of the program MOLBD. Force fields were adapted from those published by DeHayes and Busch,[34] no unusual modifications were required to approximate the angles about the capping nitrogen atoms of the sep ligand or any of the features of en. For the Co–N interactions, normal distances and Urey–Bradley force constants of 1.975 Å and 2.24 N m^{-1}, respectively, for Co(III) and 2.10 Å and 1.39 N m^{-1} for Co(II) were used. Cobalt-donor angle deformation constants given by DeHayes and Busch for Co(III) were used for both Co(III) and Co(II) since these constants are typically only 10% of the bond deformation constants and reliable estimates for Co(II) are not available. Indeed, the force field is dominated by the carbon and nitrogen atoms, with force constants typically 4 times larger than those of transition-metal ions, and these constants are, of course, effectively independent of the oxidation state of the central ion. For $Co(sep)^{3+,2+}$ 51 atoms and 529 interactions were included in the calculation; for $Co(en)_3^{3+,2+}$, 37 atoms and 305 interactions were included. A root mean square coordinate shift of 1 pm was accepted as the convergence criterion. This procedure worked well for various combinations of *ob* and *lel* chelate ring conformers.

The energy of the eclipsed ring complexes was estimated by forcing one ring into an eclipsed conformation with use of the Δ potential described by Boyd.[32] Briefly, the Δ potential is a measure of the deviation from planarity in, for example, arenes. Given sufficiently large Δ deformation constants (e.g., about 5 N m^{-1} compared with about 0.8 N m^{-1} for a typical arene), one chelate ring was forced into a planar (eclipsed) conformation; eight cycles were required to minimize the $Co(sep)^{3+}$ structure, and five cycles were required for the $Co(en)_3^{3+}$ structure. The Δ potential was then removed, "normal" torsional potential functions were restored, and the energy was calculated without permitting the coordinates to shift. All other calculations were performed with use of standard methods, which are published elsewhere.[33]

Partial Normal-Coordinate Analysis. The vibrational secular equation $|GF - E\lambda| = 0$ has been solved for A_1-type vibrations in $Co(en)_3^{3+}$ with use of Miyazawa's method.[35,36] The **G** matrix in internal coordinates was computed by using Schachtschneider's GMAT program.[37] The Cartesian coordinates for atoms in $Co(en)_3^{3+}$ were based on the same X-ray structures[38] as in the force field calculation. Coordinates were assigned to atoms of one of the en chelate rings, and the coordinates of the remaining atoms were generated by C_3 and

(31) Stein, P.; Miskowski, V.; Woodruff, W. H.; Griffin, J. P.; Werner, K. A.; Gaber, B. P.; Spiro, T. G. *J. Chem. Phys.* **1976**, *64*, 2159.
(32) Boyd, R. H. *J. Chem. Phys.* **1968**, *49*, 2574.
(33) Brubaker, G. R.; Johnson, D. W. *Coord. Chem. Rev.*, in press.
(34) DeHayes, L. J.; Busch, D. H. *Inorg. Chem.* **1973**, *12*, 1505.
(35) Miyazawa, T. *J. Chem. Phys.* **1958**, *29*, 246.
(36) Schachtschneider, J. H.; Snyder, R. A. *Spectrochim. Acta* **1963**, *19*, 117.
(37) Schachtschneider, J. H. Technical Report 231-64; Shell Development Co.: Emeryville, CA, 1964.
(38) Witiak, D.; Clardy, J. C.; Martin, D. S., Jr. *Acta Crystallogr., Sect. B: Struct. Crystallogr. Cryst. Chem.* **1972**, *B28*, 2698.
(39) Gouteron-Vaissermann, J. *C. R. Seances Acad. Sci., Ser. B* **1972**, *275*, 149.
(40) Krishanan, K.; Plane, R. A. *Inorg. Chem.* **1966**, *5*, 852.

Table I. Summary of Kinetic Data for $Co(sep)^{2+}$ Reactions

oxidant	$10^5 \times$ [$Co(sep)^{2+}$], M	$10^4 \times$ [oxidant], M	k,[a] $M^{-1}\ s^{-1}$
$Ru(NH_3)_6^{3+}$	5.0	2.5-6.0	$(3.5 \pm 0.2) \times 10^4$ (4)[b]
$Co(bpy)_3^{3+}$ [c]	6.0-120	0.06-2.0	$(1.0 \pm 0.15) \times 10^4$ (6)
$Co(NH_3)_6^{3+}$	5.0-15	20-120	0.15 ± 0.015 (9)
$Co(en)_3^{3+}$	5.0-15	30-130	0.05 ± 0.005 (8)
$Ru(NH_3)_4(phen)^{3+}$	5.0	2.5	$>10^5$ [b]

[a] Conditions: 0.2 M $NaCF_3SO_3$, (0.5-1.0) $\times 10^{-3}$ M HCF_3SO_3, 25 °C. The number of determinations is in parentheses. [b] Conditions: 0.49 M $NaClO_4$, 0.01 M $HClO_4$. [c] Pseudo-first-order conditions were employed with either reductant or oxidant in excess.

C_3^2 symmetry operations. A molecular symmetry of D_3 was used to classify the vibrations into different symmetry classes. Valence force constants were estimated by iteration to reproduce the observed frequencies.[29,37,38] To simplify the calculations, hydrogen atoms were neglected and $-CH_2$ and $-NH_2$ groups considered as point masses. As a consequence the $Co(en)_3^{3+}$ ion can be considered to have 33 vibrational modes of symmetry types $6A_1 + 5A_2 + 11E$. Alternatively these may be classified, including 18 redundant modes, as 15 stretching, 21 bending, and 15 torsional modes. Symmetry coordinates were assigned on the basis of interatomic distances (γ_i), bond angles ($\theta_{i,j}$), and atom numbers as indicated:

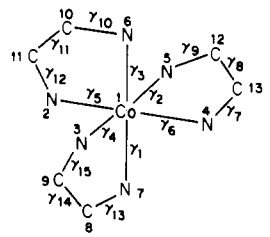

The symmetry coordinates were constructed by the projection operator method for D_3 symmetry. We have considered in the computation only the five A_1-type modes: (1) Co–N stretch, $^1/_6(\gamma_1 + \gamma_2 + \gamma_3 + \gamma_4 + \gamma_5 + \gamma_6)$; (2) C–C stretch, $^1/_3(\gamma_8 + \gamma_{11} + \gamma_{14})$; (3) C–N stretch, $^1/_6(\gamma_7 + \gamma_9 + \gamma_{10} + \gamma_{12} + \gamma_{13} + \gamma_{15})$; (4) N–Co–N bend, $^1/_{18}(2\theta_{2,6} + 2\theta_{3,5} + 2\theta_{1,4} + \theta_{1,2} + \theta_{1,5} + \theta_{2,5} + \theta_{3,4} + \theta_{4,6} + \theta_{3,6})$; (5) Co–N–C bend, $^1/_6(\theta_{5,12} + \theta_{2,9} + \theta_{1,13} + \theta_{4,15} + \theta_{6,7} + \theta_{3,11})$.

Asymmetric contributions, such as those originating in the nonbonded repulsions between organic ligands, were not taken into account in this simplified analysis but are included in the force field calculation.

Results

The analytical, spectroscopic, and electrochemical data we have obtained are in good agreement with those reported for $Co(sep)Cl_3$ by Sargeson and co-workers.[18]

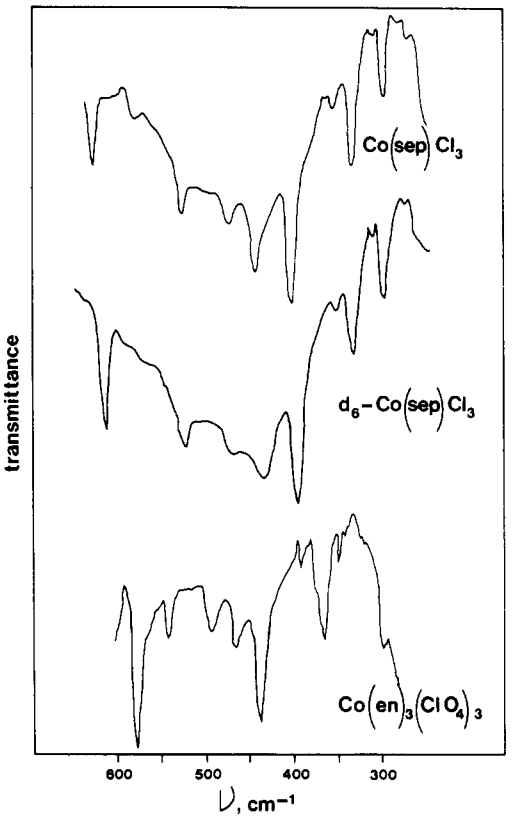

Figure 1. Far-infrared spectra (from top to bottom) of $Co(sep)(ClO_4)_3$, $Co(sep\text{-}d_6)(ClO_4)_3$ (N-deuterated), and $Co(en)_3Cl_3$.

The bimolecular rate constants obtained in this study are summarized in Table I. The reproducibility and quality of fit of pseudo-first-order rate constants were taken as the criteria for eliminating the problems due to oxygen contamination and decomposition of $Co(sep)^{2+}$.

The results of our infrared and Raman studies are summarized in Table II, and the infrared spectra of $Co(sep)^{3+}$ and $Co(sep\text{-}d_6)^{3+}$ (sep-d_6 denotes deuteration at the six nitrogens with hydrogens attached to them) are compared to the $Co(en)_3^{3+}$ spectrum in Figure 1. In addition to these spectra we have found the N–H and C–H stretching frequencies (dominant peaks at 3220, 3150, and 3095 cm^{-1} in $Co(en)_3^{3+}$) to be so shifted in $Co(sep)^{3+}$ (dominant peak at 3038 cm^{-1} and a new peak at 2850 cm^{-1} with a minimum between 3200 and 3300 cm^{-1}) that this region of the infrared can be diagnostic

Table II. Far-Infrared and Raman Spectra of Sepulchrate and Ethylenediamine Complexes[d]

$Co(sep)Cl_3$		$Co(sep\text{-}d_6)Cl_3$	$Rh(sep)_3$		$Co(en)_3Cl_3$[a]				$Rh(en)_3Cl_3$[a]			
IR	R	IR	IR	R	IR	assignt	R	assignt	IR	assignt	R	assignt
628 s		*618* s	*624* s		*578*	e_u	582	e_g	574	e_u	576	e_g
(586) w		(575) vw	(578) w									
532 m	...	*523* m	*523* m	...	*544*	a_{2u}			*542*	a_{2u}		
	520[b]						*526*	a_{1g}			*547*	a_{1g}
478 m	499 sh[b]	476 m	467 m		495	e_u	501	e_g	498	e_u	507	e_g
447 s		440 s	445 s		468	a_{2u}			452	a_{2u}		
408 s	*415* w[c]	399 s	422 s	*419* w	438	e_u	*441*	e_g	445	?	*447*	e_g
359 w	370 m[c]	(358) w	397	374 m	368	e_u	372	e_g	354	e_u	356	e_g
339 m		337 m	369	331 w			338	a_{1g}			329	a_{1g}
305 m	307 s[c]	303 m		311 s	300	e_u	313	e_g	303	e_u	305	e_g
	279 m[c]			282 m	280	?	283	a_{1g}			285	a_{1g}
	278 m[c]		280				277	e_g			260	e_g
	220 m[c]			223 m							250	e_g
	193 w[c]			197 w			207	a_{1g}			203	a_{1g}
	180 w[c]						190	e_g			190	e_g
	154 w[c]			156 w								

[a] Bands and assignments from ref 31; metal stretching frequencies in italics. [b] Excitations at 514.5 nm. [c] Excitations at 474.96 nm. [d] Abbreviations: s = strong; m = medium; w = weak; vw = very weak; sh = shoulder.

Table III. Strain Energies Estimated for the Ground States of the $Co(sep)^{3+,2+}$ and $Co(en)_2^{3+,2+}$ Couples

complex	conformer	minimized strain energy components, kJ mol^{-1} [a] R_{ij}	θ_{ij}	ϕ_{ijkl}	NB	total energy strain, kJ mol^{-1}	calcd Co-N bond lengths in each chelate ring, pm R_1	R_2	R_3
$Co(sep)^{2+}$	$(lel)_3$	10.8	54.8	42.3	13.6	122	216	216	216
	$(lel)_2ob$	12.1	59.4	41.9	14.4	128	214	216	216
	$lel(ob)_2$	16.2	58.6	44.3	19.0	138	213	214	216
	$(ob)_3$	20.1	58.5	50.2	24.8	154	213	213	213
$Co(sep)^{3+}$	$(lel)_3$	17.9	50.2	38.1	46.9	153	199	199	199
	$(lel)_2$eclip	17.2	50.2	58.0	58.0	183	199	199	199
	$(lel)_2ob$	17.9	53.5	41.8	45.2	159	199	199	200
	$lel(ob)_2$	15.1	43.1	44.8	46.4	149	199	197	197
	$(ob)_3$	14.3	33.2	51.0	53.1	152	197.5	197.5	197.5
$Co(en)_3^{2+}$	$(lel)_3$	3.7	15.0	6.5	0.7	26			
$Co(en)_3^{3+}$	$(lel)_3$	6.7	14.2	10.0	7.9	39			
	$(lel)_2$eclip	6.7	17.1	24.2	16.3	65			

[a] Interaction constants chosen to reproduce crystallographic features of $Co(en)_3^{3+}$ and $Co(sep)^{2+}$.

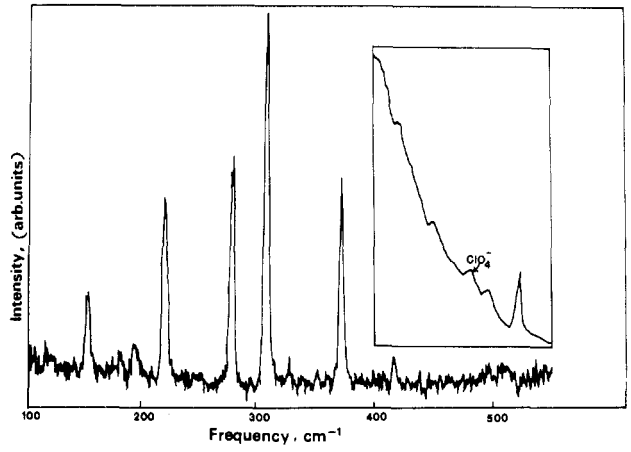

Figure 2. Raman spectrum of $Co(sep)(ClO_4)_3$ in water at 25 °C. Low-frequency lines are for laser excitation at 474.96 nm; high-frequency lines (inset) are for laser excitation at 514.5 nm.

of compound purity. The deuteration of N–H in $Co(en)_3^{3+}$ and $Co(sep)^{3+}$ was used to identify the N–H stretching frequencies. The new peak at 2850 cm^{-1} in $Co(sep)^{3+}$ is most likely attributable to the capping methine groups.

In accord with the reported[31] deenhancement of the Raman intensity of the a_{1g} breathing mode for excitations of ligand field transitions, we were unable to definitively detect Raman frequencies in the 500–550-cm^{-1} region for 475-nm excitations of $Co(en)_3^{3+}$ or $Co(sep)^{3+}$ (Figure 1). However, Raman lines in this region were observed (insert in Figure 1) for 514.5-nm excitations. A very well resolved peak appeared at 520 cm^{-1} for $Co(sep)^{3+}$, which compares well with the 526-cm^{-1} a_{1g} mode found for $Co(en)_3^{3+}$ [30] and with 526 cm^{-1} found for the a_{1g} mode of $Co(sep)^{3+}$ based on our molecular mechanics calculations. The other peaks observed in the 500-cm^{-1} region for 514.5-nm excitations of $Co(sep)^{3+}$ (insert in Figure 1) can be assigned as ν(Co–N e_g) at 415 cm^{-1}, $\nu(ClO_4^-)$ at 475 cm^{-1}, ν(ligand e_g) at 499 cm^{-1}, and ν(Pyrex) at ca. 490 cm^{-1}; all assignments are based on comparison to $Co(en)_3^{3+}$ (Table III). In contrast, 514.5-nm excitations of $Co(sep)^{2+}$ resulted in resolvable Raman lines (apart from those of ClO_4^- and Pyrex) only at 368 and 356 cm^{-1}. The absence of the 520-cm^{-1} band is consistent with the smaller force constants expected for Co(II) than for Co(III); for comparison, the a_{1g}(Co–N) modes have been assigned at 494 and 357 cm^{-1}, respectively, for $Co(NH_3)_6^{3+}$ and $Co(NH_3)_6^{2+}$.[41,42] The close correspondence of the infrared and Raman frequencies observed for $Co(sep)^{3+}$ and $Co(en)_3^{3+}$ (Table II) indicates that the Co–N force constants are very similar in these compounds.

The approximate normal-coordinate calculation (a_1-type motions only) indicates that the 526-cm^{-1} vibration of $Co(en)_3^{3+}$ originates largely in the symmetric Co–N stretching (~84% of the symmetry force constant) with a significant (~15%) contribution of the N–Co–N deformation mode. Within the limits of our treatment, none of the other molecular motions appear to contribute significantly to this vibration.

Strain energy minimization calculations were employed to estimate a total contribution of nuclear motion to the rate constant. The Newton–Raphson minimization scheme employed in our calculation establishes a Cartesian surface over which nuclei are repositioned in response to the steric demands of all other nuclei. Specifically, we consider the following terms (a, A, B, C, c are constants): $U(R_{ij}) = 0.5k(\Delta x)^2$ (bond deformation); $U(\theta) = 0.5k'(\Delta\theta)^2$ (angle deformation); $U(\phi) = 0.5k''(1 + a\cos(\phi - C))$ (torsion); $U(\mathrm{NB}) = A\exp(-B/r) + r^c$ (nonbonded interactions).

We find, for example, that changes in the Co–N distance result in substantial changes in the angle deformation and nonbonded interactions of the ethylene bridges in sep complexes, reflecting overall coupling (albeit informal since coupling constants cannot be estimated) of bond length, angle deformation, and torsional modes.

The ground-state strain energy minimization calculations have been carried out for the *ob* and *lel* conformers of $Co(sep)^{3+}$ and $Co(sep)^{2+}$ and the *lel* conformers of $Co(en)_3^{3+}$ and $Co(en)_3^{2+}$ (Table III). In addition, we have included in Table III the results of calculations on Co(III) complexes with one chelate ring in an eclipsed conformation. Our calculations indicate that the *ob* and *lel* conformers are nearly isoenergetic for $Co(sep)^{3+}$ but that the $(lel)_3$ conformer is appreciably more stable for $Co(sep)^{2+}$. In this connection, it is interesting to note that the conformer isolated for X-ray crystallographic study was $(lel)_3$-$Co(sep)^{2+}$.[18c] Our calculations also indicate that the activation energies for $ob \rightleftarrows lel$ isomerization should be comparable for $Co(en)_3^{3+}$ and $Co(sep)^{3+}$, on the basis of the similar differences in energy between the respective $(lel)_3$- and $(lel)_2$-eclipsed conformers.

In view of these calculations we have sought evidence for the presence of *ob–lel* conformational isomerization in the $Co(sep)^{3+,2+}$ system. The narrow line widths of the ^1H NMR spectra for $Co(sep)^{3+}$ suggest that the isomerization rate must be less than 10^5 s^{-1}. Even the most rapid electron-transfer reactions have had monotonic, good quality decay constants, and this would suggest an isomerization lifetime of less than 10 ms.

On the other hand, the calculated difference in stabilities of $Co(sep)^{2+}$, but not $Co(sep)^{3+}$, conformers could manifest

(41) Schmidt, K. H.; Müller, A. *Inorg. Chem.* **1975**, *14*, 2183.
(42) Mohan, N.; Cyvin, S. J.; Müller, A. *Coord. Chem. Rev.* **1976**, *21*, 221.
(43) Haupt, H. J.; Huber, F.; Preul, H. *Z. Anorg. Allg. Chem.* **1976**, *422*, 255.

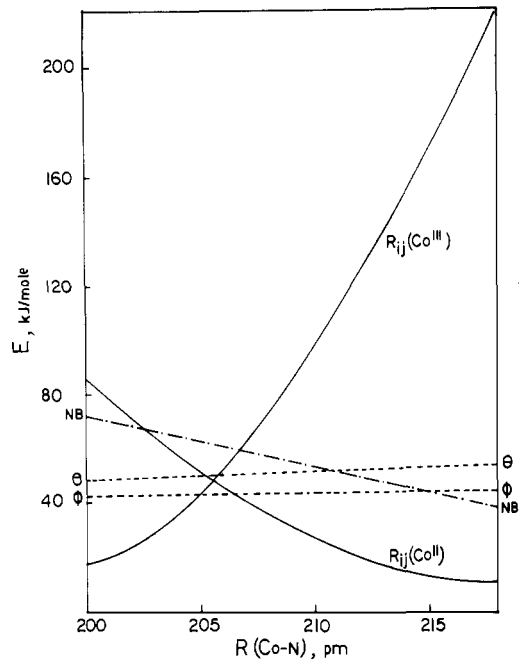

Figure 3. Variation of strain energy components with coordination sphere "hole size" for $Co(sep)^{3+,2+}$.

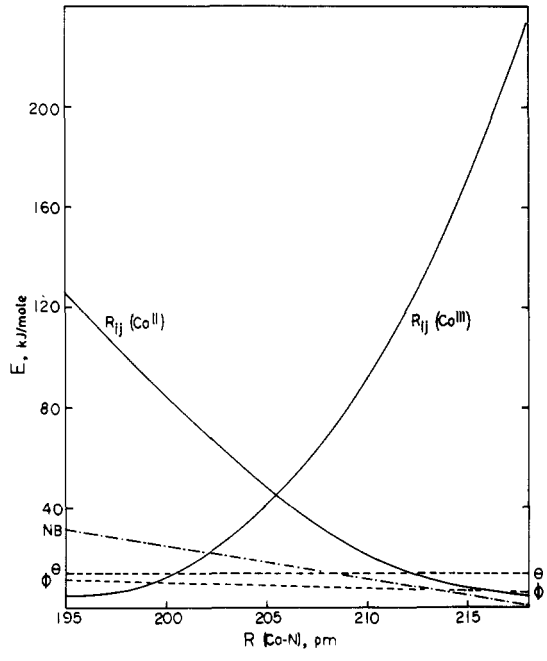

Figure 4. Variation of strain energy components with coordination sphere "hole size" for $Co(en)_3^{3+,2+}$.

itself in a shift in potential under certain conditions. We have found the $Co(sep)^{3+,2+}$ half-wave potential to be -0.54 ± 0.01 V vs SCE in 0.1 M $NaCF_3SO_3$ and -0.585 ± 0.005 V vs SCE in 0.1 M $NaCH_3CO_3$. This difference in potentials would be consistent with some stabilization of the $(ob)_3$-$Co(sep)^{3+}$ conformer in acetate media, possibly through hydrogen-bonding interactions; this would correspond to a change from about a 1:1 ratio of $(lel)_3$:$(ob)_3$ conformers in $NaCF_3SO_3$ to about a 1:6 ratio in $NaCH_3CO_3$. Further investigation of this behavior using fast-sweep (100 V s^{-1}) cyclic voltammetry in the $NaCF_3SO_3$ medium did not reveal the shifts of potential that would be expected for conformational isomerization on this time scale. On this basis we would estimate a relaxation time of less than 10^{-3} s for the conformational equilibrium.

Two approaches to the total steric contributions to the electron-transfer rate were employed. In the first, the Co–N bond length was "stepped" through several values intermediate between the published Co(II) and Co(III) values, and the calculation was allowed to converge (typically in three cycles). From these calculations, we have estimated the contributions of angle deformations, torsion, and nonbonded interactions. Our estimate of the contributions of bond deformations derives from a calculation of the bond strain of a Co(II) ion in a Co(III) site (i.e., Co(II) force constants and Co(III) distances) and a calculation of the bond strain of a Co(III) ion in a Co(II) site. Each of the four contributions to strain energy (in our model) is plotted against d(Co–N) for $Co(sep)^{3+,2+}$ in Figure 3 and for $Co(en)_3^{3+,2+}$ in Figure 4. In order to evaluate the geometry and strain energy in the transition states for electron exchange, we have had to take account of the uncertainties in Co–N distances[12,18,38,44] since the saddle point of the reaction

Table IV. Summary of Variations in $\Delta G_{in}^{\ddagger}$ with Boundary Conditions (Energies in kJ mol^{-1})

couple	R_0^{III},[a] pm	R_0^{II}, pm	$R^{\ddagger}$, pm	$\Delta G^{\ddagger}$ [b]	$\Delta G_{in}^{\ddagger} + \Delta G_{out}^{\ddagger} + w$	$\Delta G^{\ddagger}$(obsd)
$Co(sep)^{3+,2+}$	196	218	207	84.7	109	58
	199[c]	216[c]	208	47.4	71	58
	201	215	210	29.3	53	
	196[d]	218[d]	208[d]	64.4[d]	88	
$Co(en)_3^{3+,2+}$	196	218	206	83.7	110	87
	199	216	207	49.0	75	
	201	215	208	31.5	58	

[a] Range in R_0 based on range reported for Co–N distances in X-ray structure determinations. See text. [b] Except as indicated, the value of $\Delta G_{in}^{\ddagger}$ is based on the assumption that the cited values of R_0 correspond to the equilibrium Co–N distances appropriate to the choice of force constant and that this is the same as the net equilibrium Co–N distance in the complex. [c] R_0 based on reported mean Co–N distances. [d] Estimate is based on R_0 for the Co–N vibration identical with the mean bond lengths reported for $Co(en)_3$, but net equilibrium Co–N distances in the Co(sep) ions are based on the reported mean of the crystallographic values. This estimate provides the most internally consistent comparison with the $Co(en)_3^{3+,2+}$ couple (using the same boundary conditions; next entry).

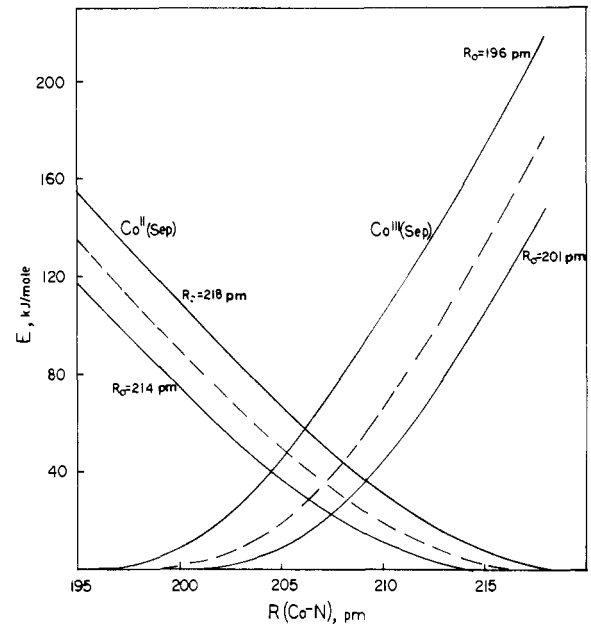

Figure 5. Variation in the Co–N stretching energy with assumed equilibrium distance (R_0). Force constants: 248 N m^{-1} (Co^{III}) and 139 N m^{-1} (Co^{II}).

(44) Duesler, E. N.; Raymond, K. N. *Inorg. Chem.* **1971**, *10*, 1486.
(45) Magill, L. S.; Korp, J. D.; Bernal, I. *Inorg. Chem.* **1981**, *20*, 1187.

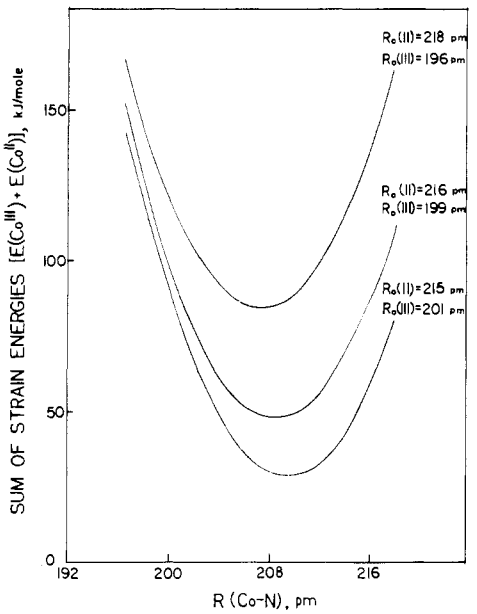

Figure 6. Variations in the saddle point energy and in R^* with variation in boundary conditions (R_0).

surface is very sensitive to the choice of R_0 for the Co–N bond deformations. This sensitivity can be most readily visualized if one examines the effect of such uncertainties on the intersections of the harmonic Co(III) and Co(II) R_{ij} components as in Figure 5. Values of R_0 used in Figure 5 or in Table IV have been selected to span the *range of individual* (not mean) *values* of Co–N bond lengths reported for $Co(en)_3^{3+}$ and $Co(sep)^{3+}$, on the one hand, and estimated for $Co(en)_3^{2+}$ and reported for $Co(sep)^{2+}$, on the other. In general the Co^{III}–N bond lengths reported in a single structure tend to deviate from the mean value by <1 pm (standard deviation). The Co^{II}–L bond lengths are generally more variable with deviations from the mean running typically ~3 pm in $Co^{II}L_6$ complexes.[12] Since the reorganizational energy goes as the square of the *difference* in Co(III) and Co(II) bond lengths, these small uncertainties in bond length necessarily translate into large uncertainties in calculated reorganizational energies. For example, for a "typical" value of $\Delta R_0 = R_0(Co^{II}–N) \approx 20$ pm, the uncertainty in ΔR_0 is between ±2 and ±4 pm, or 20–40% in the R_{ij} component of ΔG_{in}^*. This is graphically illustrated in Figure 5 with the crossing of the dashed lines representing the R_{ij} component of ΔG_{in}^* for the mean Co^{III}–N and Co^{II}–N bond lengths, while the crossing points of the solid lines represent the *range* of values possible based on variations in the structural parameters.

In order to arrive at a value of the saddle point energy for a given set of boundary conditions (i.e., values of R_0), we have minimized the total strain energy for several vaues of $d(Co^{III}–N) = d(Co^{II}–N)$ in the neighborhood of the intersections of the respective R_{ij} components (e.g., see Figures 3 and 4). The minimum of the resulting plot of minimized potential energy vs. d(Co–N) is the estimated saddle point energy (see Figure 6). The upper and lower curves in Figure 6 represent the estimated *range* of boundary conditions as discussed in the preceding paragraph. The results of the calculations are summarized in Table IV.

Discussion

Literature parameters and our data demonstrate that eq 2 adequately describes most of the variations with ΔG_{ab}° of the rates of $Co(sep)^{2+}$ reactions (Figure 7). The scatter of data in Figure 7 (mean deviations from the solid correlation line ~4 kJ mol^{-1}) originates in part in variations in media used by workers in different laboratories, and there may still be

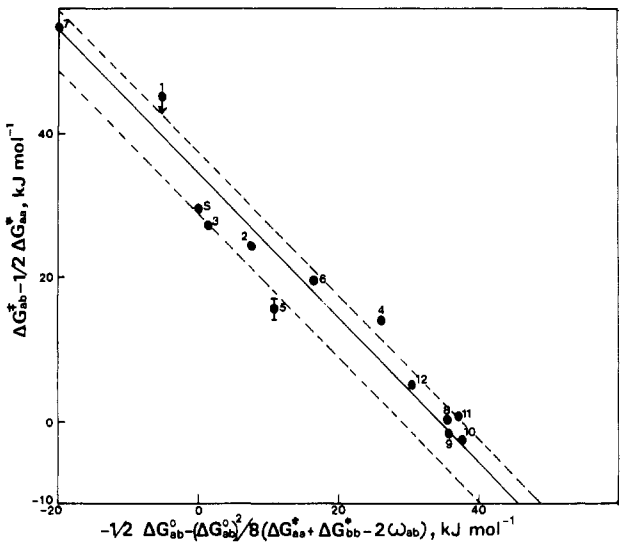

Figure 7. Dependence of rates of oxidation of $Co(sep)^{2+}$ on the free energy change. The correlation is based on eq 2. Oxidants: (1) Cr^{3+} (based on $Cr^{2+}/Co(sep)^{3+}$ and equilibrium constant[18]); (2) $Cr(Me\text{-}phen)_3^{3+}$;[29] (3) $Co(en)_3^{3+}$; (4) $Co(bpy)_3^{3+}$; (5) $Co(NH_3)_6^{3+}$; (6) $Ru(NH_3)_6^{3+}$; (7) U^{4+} (based on $U^{3+}/Co(sep)^{3+}$ and equilibrium constant[18]); (8) $Co(Me_2pyo[14]trieneN_4)(OH_2)_2^{3+}$;[10] (9) $Co(Me_4\text{-}[14]tetraeneN_4)(OH_2)_2^{3+}$;[10] (10) $Co(Me_2[14]4,7\text{-}dieneN_4\text{-}13\text{-}one)\text{-}(OH_2)_2^{3+}$;[10] (11) $Co(Me_6[14]4,11\text{-}dieneN_4)(OH_2)_2^{3+}$;[10] (12) $Co\text{-}([14]aneN_4)(OH_2)_2^{3+}$.

some contributions from the acid instability of $Co(sep)^{2+}$.[18c] It is also possible that some of this scatter originates from differing contributions of electronic terms to the various reactions. Thus, points representing the electronically similar (in the sense of electronic configurations and excited-state energies) reactions $Co(sep)^{3+,2+}$, $Co(en)_3^{3+}/Co(sep)^{2+}$, and $Co(NH_3)_6^{3+}/Co(sep)^{2+}$ are below the correlation line in Figure 7. As a consequence, the rate constants for these reactions are about 10 times larger than one would predict on the basis of the remaining cross-reactions. Equation 1 is certainly not readily factored into separate electronic contributions of donor and acceptor, and the λ parameters in the quadratic term of eq 2 represent only Franck–Condon contributions, so one would not expect an exact fit of eq 2 to a large variety of reactions when electronic terms do make significant contributions. The sense of the deactivation is suggestive of a larger exchange contribution to the electronic matrix element for the electronically similar donor–acceptor combinations. The effect reported here is small, the uncertainties are large, and these observations do not permit a definitive statement. However, observations reported elsewhere[7b,46] do lend support to a significant exchange contribution to the electronic matrix element in reactions of this class. A consequence of such contributions is that self-exchange reactions will generally tend to be more adiabatic than cross-reactions, a point that we have noted elsewhere.[11]

While there are a number of differences of detail in the infrared spectra of $Co(en)_3^{3+}$ and $Co(sep)^{3+}$ in the regions appropriate to CH_2 deformation modes, much more striking are the shifts of the N–H and C–H stretching frequencies to lower energy in the latter complex. This seems in part a manifestation of the much greater nonbonded repulsions between methylene groups in $Co(sep)^{3+}$ than in $Co(en)_3^{3+}$; thus this shift provides a very nice qualitative confirmation of this aspect of the strain energy calculation.

In contrast, it is clear that the far-infrared and Raman spectra of $M(sep)^{3+}$ and $M(en)_3^{3+}$ (M = Co, Rh) complexes

(46) Ramasami, T.; Endicott, J. F., work in progress.

are very similar in the correspondence of bands, in band shape, and even approximately in band energy. We have used this remarkable correspondence as the basis for assigning frequencies. The a_{1g}-like breathing modes in $Co(sep)^{3+}$ and $Co(en)_3^{3+}$ differ little in energy, with the breathing mode of $Co(sep)^{3+}$ ~6 cm^{-1} lower in energy. In contrast the asymmetric stretch (averaging the e_u and a_{2u} components) averages ~30 cm^{-1} higher in energy for $Co(sep)^{3+}$ than for $Co(en)_3^{3+}$. These small shifts are plausibly attributed to coupling of Co–N and N–C motions, with signs of the coupling force constants being opposite for the breathing (and symmetric stretching) modes than for the asymmetric stretching mode.

The activation free energies for the $Co(sep)^{3+,2+}$ and $Co(en)_3^{3+,2+}$ self-exchange reactions are 58 and 87 kJ mol^{-1}, respectively. Since, in the harmonic oscillator approximation, the first coordination sphere reorganizational energy increases as ν^2,[2-6,24] to attribute the differences in self-exchange rate simply to differences in force constants would require an 18–20% difference in values of the critical vibrational frequencies. It is clear that there are no such large frequency variations among these cobalt(III) complexes. Consequently, we cannot support the earlier speculation[10,25,47] that the large difference in $Co(en)_3^{3+,2+}$ and $Co(sep)^{3+,2+}$ self-exchange rates originates from large differences in the respective Co–N stretching force constants. In fact much (~60%) of this difference in reactivity can be attributed to the reported differences in Co^{III}–N and Co^{II}–N bond lengths.

Unfortunately, such very simple discussions of the first-coordination-sphere reorganizational energies are bound to be misleading owing to the very complicated coupling between Co–N and internal ligand motions in these molecules. In this context, there are two related issues that must be considered: (a) Which changes in nuclear coordinates result in the minimum energy pathway leading from reactants to products? (b) How does one relate the normal coordinates that fit the molecular vibrational spectrum to coordinates involved along this minimum energy trajectory on the reaction surface? Our strain energy minimization calculations are an approach to the first issue. The second is far more complex, and we have only partial answers at this time.

As a general rule one cannot expect that those atomic motions that couple in the normal modes appropriate to the vibrational spectrum in complex molecules will correspond to coupled atomic motions along the minimum energy trajectory of the reaction coordinate in configuration space. For example, our partial normal-coordinate analysis suggests some coupling between the Co–N stretching and N–Co–N deformation motions. While the Co^{III}–N and Co^{II}–N bond lengths differ appreciably,[24] the evidence at hand (X-ray structures of $Co(en)_3^{3+}$ [38,43-45] and $Ni(en)_3^{2+}$ [48] and the strain energy minimization calculations) does not support any significant variations in N–Co–N bond angles. In fact, it appears that the N–Co–N angles are about 88° in both Co(III) and Co(II), with these angles being maintained within the chelate rings at the expense of low-energy torsional strain. Consequently, it appears that the vibrational normal coordinates cannot be simply related to the changes in nuclear coordinates that accompany electron exchange in such a complex molecule, and it is not appropriate to use $F_{a_{1g}}$ in calculations of $\Delta G_{in}^{\ddagger}$ for $Co(en)_3^{3+,2+}$ or for $Co(sep)^{3+,2+}$. Our strain energy minimization calculations have been performed on the $(lel)_3$ conformers using the same force constants and equilibrium bond lengths for similar bonds in $Co(en)_3$ and Co(sep). This constraint poses no conceptual difficulties for motions of atoms within the chelate ligands since the parameters for the pertinent interactions are well established. The metal–ligand force constants and equilibrium distances are a more serious problem since the observed Co–N distances differ with the ligand. In our calculations we have assumed that the Co^{III}–N and Co^{II}–N stretching force constants are *not* dependent on the ligand. Thus, we have used $F_{a_{1g}}$ force constants appropriate to $Co(NH_3)_6^{3+}$ and $Co(NH_3)_6^{2+}$, respectively.[41,42,49] We have further assumed that the Co–N bond lengths observed in the actual complex are the result of an equilibrium between the Co–N force field (which tends to force a bond length, R_0, at which the potential energy of the Co–N interaction is minimized) and interligand (or intraligand) interactions that tend on balance to alter the size of the coordination sphere cavity. As a consequence of the competing forces the observed Co–N bond lengths do not necessarily correspond to the "equilibrium" value of R_0 for the specific choice of Co–N force constants (a choice that is independent of inter- and intraligand interactions). Figures 5 and 6 demonstrate clearly the strong dependence of $\Delta G_{in}^{\ddagger}$ on the numerical value assumed for R_0 of the metal–ligand stretching frequencies. This results in very large uncertainties in the calculated values of $\Delta G_{in}^{\ddagger}$ as noted in Table IV and discussed above. The error limitations noted in Table IV are a necessary consequence of uncertainties in the structural information available at this time. Consequently, the best possible calculated values of self-exchange rate constants for Co(III)–Co(II) couples have intrinsic uncertainties that are at the very best on the order of a factor $10^{0\pm2}$ in the rate constant. Since Co^{II}–L bond lengths seem to be more variable than ±1 pm, and since force constants (obtained by fitting spectra or potential energy surfaces in the insensitive region of small displacements, that is, $f = \partial^2 V/\partial R^2$ evaluated at R_0, and based on simple force field models) are also subject to uncertainties, we believe that this is a conservative estimate of the errors intrinsic to calculated Franck–Condon parameters.

While the calculated contributions to $\Delta G_{in}^{\ddagger}$ are subject to considerable uncertainty, estimates of the variation in $\Delta G_{in}^{\ddagger}$ for a series of closely related compounds might be more reliable. In our comparison of the $Co(en)_3^{3+,2+}$ and $Co(sep)^{3+,2+}$ couples (Table IV) we have estimated $\Delta G_{in}^{\ddagger}$ for a range of boundary conditions based on the observed variation of Co–N bond lengths determined by X-ray crystallography. Since the input parameters used are the same for both couples, identical sets of boundary conditions (i.e., identical values of ground-state Co–N bond lengths) lead to very similar (±2 kJ mol^{-1}) values of $\Delta G_{in}^{\ddagger}$ for these complexes. However, if one assumes identical R_0 values for the Co–N vibrations (i.e., R_0 = 196 pm for Co^{III}–N and R_0 = 218 pm for Co^{II}–N), identical force constants and assumes that some coordination sphere expansion of $Co(sep)^{3+}$ and compression of $Co(sep)^{2+}$ results from intraligand forces, as implied by the X-ray structural data for these complexes, then the calculated contributions for the $(lel)_3$ conformers (lines 4 and 5 in Table IV) differ by 22 kJ mol^{-1} in good agreement with experimental observation (28 kJ mol^{-1}). For exchange between the $(ob)_3$ conformers, $\Delta G_{in}^{\ddagger}$ would be ~20% smaller for $Co(sep)^{3+,2+}$; however, the apparently greater stability of the $(lel)_3$ conformer[50] of $Co(sep)^{2+}$

(47) It should be noted that while Geselowitz[25] speculated that these differences in $\Delta G_{exch}^{\ddagger}$ arose from differences in the respective ligand strain energies, the specific model proposed by him necessarily results in a larger stretching force constant for Co(sep) than for $Co(en)_3$. The difference in activation barriers calculated by Geselowitz results from the ~20% difference reported for Δd(Co–N) in the two complexes (17 and 21 pm, respectively[25]). This difference in bond lengths accounts for ~60% of the difference in $\Delta G_{in}^{\ddagger}$ if the Co–N force constants are assumed to be the same and no other factors contribute.

(48) Cramer, R. E.; Doorne, W. V.; Huneke, J. H. *Inorg. Chem.* **1976**, *15*, 529.

(49) Note that this transference of metal–ligand force constants is consistent with about 85% of the 526-cm^{-1} frequency arising from metal–ligand stretching motions.

Table V. Comparison of Estimated Franck-Condon Contributions to Several Co(III)-Co(II) Self-Exchange Couples

couple	R_0^{III},[a] pm	R_0^{II},[a] pm	Co^{III}-N,[b] pm (range, 2σ)	Co^{II}-N,[b] pm (range, 2σ)	f_{III}, N m^{-1}	f_{II}, N m^{-1}	ΔG_{in}(calcd),[c] kJ mol^{-1}	$\Delta G^{\ddagger}$(calcd),[c] kJ mol^{-1}	$\Delta G^{\ddagger}$(obsd), kJ mol^{-1}
$Co(en)_3^{3+,2+}$	196	218	196 (195-198, 1)[d]	217 (218,[e] $2\sigma \geq 1$)	248	139	58 ± 14 (c) 53 ± 14 (q)	84 ± 14 (c) 79 ± 14 (q)	87
$Co(sep)_3^{3+,2+}$	196	218	199 (199,[f] 1)	215 (215-218, 2)[f]	248	139	38 ± 10[g] (c) 33 ± 10 (q)	52 ± 10 (c) 47 ± 10 (q)	58
$Co(OH_2)_6^{3+,2+}$	190	210	190 (187[h]-191[i], ~1)	210 (206-213, 3)[j]	254	132	66 ± 29 (c) 60 ± 20 (q)	100 ± 20 (c) 94 ± 20 (q)	125[k]
$Co(NH_3)_6^{3+,2+}$	197	216	197 (196-198, 1)[l]	216 (216 ± 1)[m]	248	130	55 ± 12 (c) 50 ± 12 (q)	86 ± 12 (c) 81 ± 12 (q)	106,[k] ≤102[n]
$Co(Me_4[14]tetraeneN_4)(OH_2)_2^{3+,2+}$	191[o]	229[o]	191 (191, 1)[p]	229 (229, 2)[q]	215	61	41 ± 8 (c) 40 ± 8 (q)	58 ± 8	70[p]

[a] Current "best estimates" for boundary conditions. R_0 value is for Co-N equilibrium, with respect to the force constant indicated, and for no other forces acting to perturb this equilibrium. [b] Net equilibrium value assumed in calculation. [c] Classical barriers are designated (c); those corrected for vibrational quantization are designated (q); see ref 44. $\Delta G_{ab}^{\ddagger} = \Delta G_{in} + \Delta G_{out} + w$. [d] References 38, 43, 44. [e] XFAS determination cited in ref 25. [f] Cited in ref 18. [g] Based on the comparison to $Co(en)_3^{3+,2+}$ (Table IV) using identical input parameters. [h] Cited by: Hush, N. *ACS Symp. Ser.* **1982**, *No. 198*, 301. [i] Based on $Co(Me_4[14]tetraeneN_4)(OH_2)_2^{3+}$.[10] [j] McCandlish, E. F. K.; Michael, T. K.; Neal, J. A.; Lingafelter, E. C.; Rose, N. J. *Inorg. Chem.* **1978**, *17*, 1383. [k] Intercept of linear free energy correlation in ref 11. [l] Based on: (i) Iwata, M. *Acta Crystallogr., Sect. B: Struct. Crystallogr. Cryst. Chem.* **1977**, *B33*, 59. (ii) Iwata, M.; Saito, Y. *Ibid.* **1973**, *B29*, 822. (iii) Kruger, G. J.; Reynhardt, E. C. *Ibid.* **1978**, *B34*, 915. [m] Attributed to: Freeman, H. C. In ref 18c. [n] Reported by H. Taube at the 183rd National Meeting of the American Chemical Society, Las Vegas, Nv, March 1982. [o] Comments: Axial bonds only; equatorial bond lengths are the same in Co(III) and Co(II); low-spin Co(II); chosen as "typical" of macrocyclic cobalt(III)-cobalt(II) complexes. [p] Reference 10. Force constants are estimates based on a bond length correlation. [q] Endicott, J. F.; Lilie, J.; Kuszaj, J. M.; Ramaswamy, B. S.; Schmonsees, W. G.; Simic, M. G.; Glick, M. D.; Rillema, D. P. *J. Am. Chem. Soc.* **1977**, *99*, 429.

complicates comparisons, and since the values of $\Delta G_{in}^{\ddagger}$ for the various conformers appear to fall within the range of estimated uncertainties in any of the calculations, more detailed consideration of the reactivity differences between the conformers does not seem warranted.

In a detailed analysis, the difference in $\Delta G_{in}^{\ddagger}$ for the $Co(en)_3^{3+,2+}$ and $Co(sep)^{3+,2+}$ couples is largely a consequence of the apparent differences in Co–N bond lengths with a smaller contribution (~6 kJ mol^{-1}) originating in a greater relaxation of nonbonded repulsions for the expansion of the $Co(sep)^{3+}$ coordination sphere than for $Co(en)_3^{3+}$ coordination sphere. It is important to note that relaxation of nonbonded repulsion does make a contribution to both of these couples but that it cannot be a factor in the $Co(NH_3)_6^{3+,2+}$ self-exchange. This contribution should result in roughly a 1 order of magnitude smaller self-exchange rate for $Co(NH_3)_6^{3+,2+}$ than for $Co(en)_3^{3+,2+}$.

As noted in Tables IV and V, our best estimate of $\Delta G^{\ddagger}$, with ~5 kJ mol^{-1} for the effects of vibrational quantization[3,4d,51] at 25 °C, for the $Co(en)_3^{3+,2+}$ couple is 79 ± 12 kJ mol^{-1}. This is clearly in satisfactory accord with the experimental value of $\Delta G^{\ddagger}$ = 87 kJ mol^{-1}. However, as seems to be the case with most Co(III)–Co(II) couples,[10-12] the calculated contributions to $\Delta G^{\ddagger}$ based on Franck–Condon factors alone are slightly smaller than the observed activation barrier to self-exchange. While the discrepancies are generally within the limits of uncertainty noted above (≲20 kJ mol^{-1}), the calculated values of $\Delta G^{\ddagger}$ are systematically too small rather than being scattered randomly around the expected values. Furthermore, the harmonic models, quantized or not, are bound to overestimate $\Delta G_{in}^{\ddagger}$ since the reorganizational process corresponds to many quanta in the critical frequencies and anharmonicities are likely to play a significant role; e.g., with use of a Morse potential function and ~40 kJ mol^{-1} for Co^{III}–NH_3 dissociation in water, it is easily shown that the harmonic estimate of $\Delta G_{in}^{\ddagger}$ could be ~10% too large.[51,52] A possible source of the discrepancy is in a small value ($\sim 10^{-4\pm2}$) of the "transmission coefficient" (or electronic term ν^2) resulting from poor donor–acceptor overlap.[5] Some direct experimental probes of this factor are becoming available,[5,7,46] and future work may document this remaining component of Co(III)–Co(II) self-exchange reactions. At the present time it is clear that Franck–Condon factors compose 75–90% of the observed activation barriers and that there are no large contributions originating from the changes in spin multiplicity that accompany electron transfer.

Acknowledgment. We are grateful to Professor A. M. Sargeson for providing us with a copy of the report of the $Co(sep)^{2+}$ structure prior to its publication. We also acknowledge the assistance of Professors W. M. McClain and E. Bicknell-Brown in obtaining the Raman spectra.

(50) Sargeson and co-workers[26] have made some preliminary reports of a related strain energy minimization calculation. As far as we can ascertain, this calculation used somewhat different conventions in selecting vibrational and structural parameters. A reviewer has also pointed out that the calculation reported in ref 26b implied that dominant conformers of both $Co(sep)^{3+}$ and $Co(sep)^{2+}$ in solution have all three NCH_2CH_2N chelate rings in the *ob* conformation and that electron exchange occurs between these $(ob)_3$ conformers. This differs from our result for $Co(sep)^{2+}$.

(51) The classical inner-sphere reorganizational energy is given by[2,10,19]

$$\Delta G_{in}^{\ddagger} = \frac{n}{2}\frac{f_{III}f_{II}}{f_{III}+f_{II}}\Delta X^2$$

where f_i = appropriate force constants of the +3 and +2 ions and ΔX = change in bond length of n bonds. The corresponding expression for a vibrationally quantized system is[4d]

$$\Delta G_{in}^{\ddagger}/RT = \frac{2\nu_{III}\nu_{II}nM(\Delta X)^2/\hbar}{\nu_{III}\coth\gamma_{II} + \nu_{II}\coth\gamma_{III}}$$

where M = ligand mass, $\gamma_i = \hbar\nu_i/4k_BT$, and ν_i = activating vibrational frequencies of +3 and +2 ions.

(52) For X, the transition-state configuration coordinate, with the first three terms kept in the Taylor expansion of the exponential

$$\Delta G_{in}^{\ddagger} \simeq \frac{f}{2}\Delta X^2\left(1 - \frac{a}{2}X + \frac{a^2}{6}X^2\right)^2$$

For a mean frequency of ~400 cm^{-1}, $f \approx 160$ N m^{-1} and the anharmonicity factor $a \approx 1.8 \times 10^{10}$ m^{-1}. With these parameters the quantity in parentheses is 0.84.